The analysis for the acceleration data of vehicle running on over 100 bridges based on SSMA

Yuta Takahashi[1], Naoki Kaneko[2], Masaki Sakai[2], Ryota Shin[2], Kyosuke Yamamoto[2]

[1] Yachiyo Engineering Co.Ltd, Taito, Tokyo, Japan.
[2] University of Tsukuba, Tsukuba, Ibaraki, Japan.
yt-takahashi@yachiyo-eng.co.jp

Abstract. The advent of IoT will create a digital twin of real infrastructure on Cyber Physics System. However, installing and controlling a large number of sensors is a cost-labor. Against, there is a method of estimating bridge vibration by installing sensors on vehicle instead of installing sensors on the bridge. This method has highly mobility and agility, and it can collect big data before perfect installation of sensors on bridges. However, the accuracy of the obtained bridge features decreases, it should be analyze by data driven method with big data. While Deep Neural Network is a great solution for big data analysis, it has poor explainability. This study focuses on screening techniques by signal processing. SSMA (Spatial Singular Mode Angle), which is one of the bridge screening indexes based on mechanics, was calculated from the data of repeatedly traveling over more than 100 various bridges. The scatter plot of bridge length and SSMA has a large tendency as shown in previous studies. This trend can be used for detection of outlier which may equal change of bridge length, and this detection method can be improved by variance suppression filter in previous study or may provide the explainability based on mechanics for the result of deep learning method.

Keywords: Drive-by inspection, On-going Monitoring, Vehicle Response Analysis, Spatial Singular Mode Angle (SSMA)

1 Background of Bridge Screening by Drive-by Inspection

1.1 The necessary of digital twin bridge

Digital twin of infrastructure has a capacity to realize the data driven maintenance, the prediction of several future status and co-creation of new value with a different fields engineer. For example in Japan, the regular inspection for bridge can use drone or sensors instead of only direct visual method since 2022. The drone can capture the anomaly on surface with a detail by making 3D models and the sensors can detect the damage

within the structure. 3D models with mechanical signal data (acceleration, temperature and etc…) which is often called as Cyber-Physical System can estimate the equation of motion. With time going, the change can be extrapolated, and the several future can simulate. Data gained from digital models and real can be provide the explainability to the data analysis using AI such as DNN, RNN and Reinforced Learning. This explainability is shared with the civil engineer and data analyst, and can promote the innovation. Thus, Digital Twin of infrastructure can be "common language" for engineers. Especially, this study tries to construct the digital twin of bridges.

The number of bridge is often larger than the other infrastructures and the measurement should be cost-saver. Drone flight is often disturbed by weather conditions or regulations. For the detection of structural damage, sensors has a potential, however, the sensor putting on bridge directly may be cost-labor. The installation cost can be expensive with sensor increasing and the wireless sensors has a trade-off about the power capacity and the performance (contains sample rate, data sending and etc...). Although the sensor on bridge is ordinary at age of IoT, the sensing with ease are necessary in the dawn of construction and practical use of Digital Twin bridges. This study focuses on Vehicle Response Analysis (VRA) and the screening technology by them.

1.2 VRA

VRA is carried out by the data measured by sensors on the vehicle going over bridges. The data is analyzed based on Vehicle-Bridge Interaction (VBI) system and the change by bridge damage are detected. Generally, the damage index for bridge uses the natural frequency or the mode shape. Natural frequency (NF) is related to rigidity of the structure [1-2]. The change in little damage are small and noisy, thus it should be detect by high accuracy accelerometer. Mode shape is considered to be more robust to noise than NF [3-4]. However, bridge mode shape estimated from vehicle vibration is not accuracy. Thus, VRA is used for bridge screening.

1.3 Screening by Drive-by Inspection Technology

Drive-by bridge inspection is carried out by going vehicle with sensors. If bridge inspection is carried out by sensor data on vehicle only, the extreme high performance and huge data for supplement of the accuracy are necessary. On-going Monitoring can gather the data periodically. Screening aims the detection of data anomaly in wide area efficiently, and it doesn't need many high accurate expensive sensors. The index of bridge screening must be sensitive and robust to noise, and mode shape is often used in numerical simulation. This study uses Spatial Singular Mode Angle (SSMA) [5]. SSMA is a damage index for bridge screening and previous studies propose practical use methods [6-8]. However, the generality to the bridge environment or mechanical parameter was not enough.

1.4 The Purpose and Contribution of This Study

This study carried out the experiment to 108 bridges under the management of local government in Japan, and the trend of their SSMA are verified. The result suggests that

the bridge length – SSMA has a trend, and it shows the probability of detection without past data by direct visual inspection or measurement.

2 Vehicle-Bridge Interaction Theorem

The mathematical theorem of SSMA is shown. Calculation needs vibration and position at the front, rear axles of vehicle. The vibration should be obtained from mass points under the spring. The assumed vehicle (Half Car) model is shown in Fig. 1. This model has a rigid body as sprung-mass system, of which mass is m_s, and of which inertia moment is I_s. The point G indicates the centre of gravity, and the distances from the point G to the front and the rear axles are L_1 and L_2, respectively. In this Fig. 1, it is noted that L_1 and L_2 described as if as equal, however they are ordinary different because the engine often put near front wheel. The subscript i (= 1, 2) represents the front and rear axles. $z_{si}(t)$ and $z_{ui}(t)$ are the vertical displacements of the sprung-mass and the unsprung-mass. $u_i(t)$ is the forced displacement input under the i-th axle. k_{si} and c_{si} are the spring stiffness and the damping of the spring-mass at the i-th axle. m_{ui}, k_{ui} and c_{ui} are the mass, spring stiffness and damping of the unsprung-mass at the i-th axles, respectively. The equation of motion of the vehicle can be described by the following.

$$\mathbf{M}_{\mathrm{V}}\ddot{\boldsymbol{z}}(t) + \mathbf{C}_{\mathrm{V}}\dot{\boldsymbol{z}}(t) + \mathbf{K}_{\mathrm{v}}\boldsymbol{z}(t) = \mathbf{C}_{\mathrm{P}}\dot{\boldsymbol{u}}(t) + \mathbf{K}_{\mathrm{P}}\boldsymbol{u}(t) \tag{1}$$

respectively. ($\dot{}$) and ($\ddot{}$) denote the first-order and second-order time differentiation.

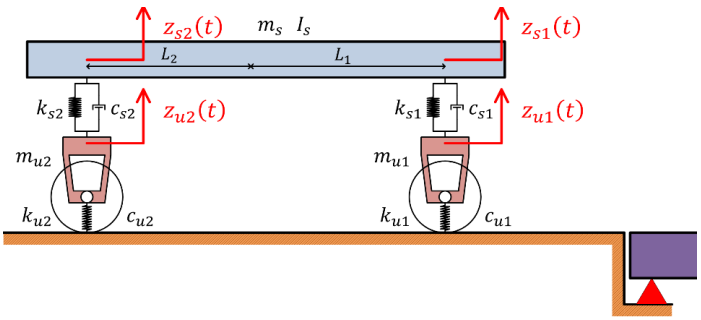

Fig. 1. Vehicle (Half Car) Model.

Since the number of sensors are same with that of estimated mode shapes, when we set a sensor on each axle, only the first and second modes can be obtained. When we use only lower mode shapes, their variation can be explained only from two factors: the measurement environment and the structural change. The latter is, in other word, a damage. On the other hand, when we use more sensors, the main factor of variation becomes the ill condition problem, which means that the results depend only on noise, not on the status of the structure. On the other hand, the bridge displacement at position x and time t can be decomposed as follows:

$$y(x,t) = \sum_k \phi_k(x) q_k(t) \tag{2}$$

$\phi_k(x)$ is the k-th order mode shape, and $q_k(t)$ is the k-th order basis coordinates. Substituting each axle position $x_i(t)$ into Eqs (2), the bridge displacement just under the i-th axle is shown below:

$$y_i(t) = \sum_k \phi_k\big(x_i(t)\big) q_k(t) \tag{3}$$

Assuming that the road roughness at the position of x is $R(x)$, the input component of the i-th axle of the vehicle at the time of t is shown below:

$$r_i(t) = R\big(x_i(t)\big) \tag{4}$$

Then, the forced displacement inputs can be described by

$$\boldsymbol{u}(t) = \boldsymbol{y}(t) + \boldsymbol{r}(t) \tag{5}$$

On the other hand, assuming that

$$\boldsymbol{\Phi}(t) = \begin{bmatrix} \phi_1\big(x_1(t)\big) & \phi_2\big(x_1(t)\big) \\ \phi_1\big(x_2(t)\big) & \phi_2\big(x_2(t)\big) \end{bmatrix} \tag{6}$$

$$\boldsymbol{q}(t) = \begin{Bmatrix} q_1(t) \\ q_2(t) \end{Bmatrix} \tag{7}$$

Eqs. (5) can be rewritten in

$$\boldsymbol{u}(t) = \boldsymbol{\Phi}(t)\boldsymbol{q}(t) + \boldsymbol{r}(t) \tag{8}$$

Next, $\phi_k\big(x_i(t)\big)$ can be discretized by interpolation as below:

$$\phi_k(x) = \sum_{j=1}^{n} a_{jk} N_j(x) \tag{9}$$

When the base function $N_j(x)$ is the Lagrangian function, the coefficient a_{kj} indicate

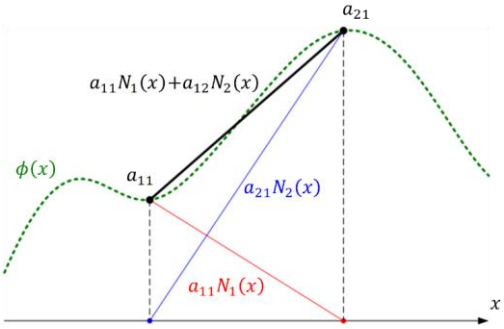

Fig. 2. Concept of interpolation.

the amplitude of k-th order mode shape at the discretized position x_j. Fig. 2 shows the concept of this interpolation.

When $n = 2$ and $x_1 = L/3$ and $x_2 = 2L/3$, the Lagrangian function is

$$N_1(x) = -\frac{3}{L}x + 2$$
$$N_2(x) = \frac{3}{L}x - 1 \tag{10}$$

$$\begin{bmatrix} \phi_1(x_1(t)) & \phi_2(x_1(t)) \\ \phi_1(x_2(t)) & \phi_2(x_2(t)) \end{bmatrix} = \begin{bmatrix} N_1(x_1(t)) & N_2(x_1(t)) \\ N_1(x_2(t)) & N_2(x_2(t)) \end{bmatrix} \begin{bmatrix} a_{11} & a_{12} \\ a_{21} & a_{22} \end{bmatrix} \tag{11}$$

By using Eqs. (10) and Eqs. (11), Eqs. (9) becomes

$$\mathbf{\Phi}(t) = \mathbf{N}(t)\mathbf{A} \tag{12}$$

where the (k, j) component of the matrix $\mathbf{A}$ is a_{kj}. Assuming that the unsprung-mass parameters of the front and rear axles are same, which means that $k_{u1}/m_{u1} = k_{u2}/m_{u2} = k_u/m_u$ and $c_{u1}/m_{u1} = c_{u2}/m_{u2} = c_u/m_u$, the vertical acceleration vibrations of the unsprung-mass can be described by

$$\ddot{\boldsymbol{z}}_u(t) = \begin{Bmatrix} \ddot{z}_{u1}(t) \\ \ddot{z}_{u2}(t) \end{Bmatrix} = \mathbf{N}(t)\mathbf{A}\boldsymbol{\sigma}(t) + \bar{\boldsymbol{\epsilon}}(t) \tag{13}$$

If the position of each axle $x_j(t)$ are available, the interpolation matrix $\mathbf{N}(t)$ can be calculated. Since the unsprung-mass vibrations $\ddot{\boldsymbol{z}}_u(t)$ and the interpolation matrix $\mathbf{N}(t)$ are known, we obtain

$$\mathbf{N}^{-1}(t)\ddot{\boldsymbol{z}}_u(t) = \mathbf{A}\boldsymbol{\sigma}(t) + \boldsymbol{\epsilon}(t) \tag{14}$$

$$\boldsymbol{\epsilon}(t) = \mathbf{N}^{-1}(t)\bar{\boldsymbol{\epsilon}}(t) \tag{15}$$

The left side of Eqs. (14) is the spatial correction of vehicle vibrations. Based on Eqs. (14), the mode shape $\mathbf{A}$ can be estimated by SVD (Singular Value Decomposition) of $\mathbf{N}^{-1}(t)\ddot{\boldsymbol{z}}_u(t)$. By SVD, the mode shape $\mathbf{A}$ and the bridge vibration component $\boldsymbol{\sigma}(t)$ are calculated at the same time. The bridge components includes only information about the bridge vibration and unsprung-mass characteristics of the vehicle. Others are included in the error term $\boldsymbol{\epsilon}(t)$: the vehicle responses: $\boldsymbol{z}(t)$, $\dot{\boldsymbol{z}}(t)$ and the road roughness: $\boldsymbol{r}(t)$ and $\dot{\boldsymbol{r}}(t)$. Since $\mathbf{N}^{-1}(t)\ddot{\boldsymbol{z}}_u(t)$ is time function, it can be described as data matrix $\mathbf{D} \in R^{2\times T}$. T means the number of the measured data. The SVD of $\mathbf{D}$ is described by the product of an orthogonal matrix $\mathbf{U} \in R^{2\times 2}$, a diagonal matrix $\mathbf{\Sigma} \in R^{2\times 2}$ and an orthogonal matrix $\mathbf{V} \in R^{T\times 2}$ ($\mathbf{V}^{\mathrm{T}}\mathbf{V} = \mathbf{I}$: the unit matrix) as below:

$$\mathbf{D} = \mathbf{U}\mathbf{\Sigma}\mathbf{V}^{\mathrm{T}} \tag{16}$$

where $\mathbf{U}$ is the estimation of $\mathbf{A}$, and $\mathbf{\Sigma}\mathbf{V}^{\mathrm{T}}$is the estimation of $\boldsymbol{\sigma}(t)$ in the form of data matrix. In order for SVD of $\mathbf{D}$ to accurately estimate the bridge mode shape $\mathbf{A}$, the following conditions need to be satisfied: (a) $\boldsymbol{\sigma}(t)$ is uncorrelated, (b) Error term $\boldsymbol{\epsilon}(t)$ is white noise. The bridge vibration components $\boldsymbol{q}(t)$ and $\dot{\boldsymbol{q}}(t)$ are transient responses induced by the traffic loads, in this case. Thus, it is considered that the real values of $\boldsymbol{\sigma}(t)$ does not satisfy the condition of a). While the SVD process gives the estimated bridge vibration components $\mathbf{\Sigma}\mathbf{V}^{\mathrm{T}}$, they are just uncorrelated signals near $\boldsymbol{\sigma}(t)$. The error due to this affects on the estimated mode shape $\mathbf{U}$. This means that the estimation mode shape $\mathbf{U}$ and the succeeding index SSMA deviate slightly from the correct mode shape.

This effect on SSMA, however, can be expected to be unchanging under the same measurement condition. Generally, a local damage on a bridge never influence the dynamic indices of the global system of the structure. Thus, it is expected that **A** remains unchanged even after the damage. However, because the local bridge responses are easily affected by the damage, the component $\boldsymbol{\sigma}(t)$ changes. The estimation for it is $\mathbf{\Sigma V}^{\mathrm{T}}$ and it cannot trace the transition. This error is included in the error of **U**. This is the mechanism of SSMA to react a bridge's local damage. The error term $\boldsymbol{\epsilon}(t)$ does not include the bridge vibrations, but the vehicle vibrations $\boldsymbol{z}(t)$, $\dot{\boldsymbol{z}}(t)$ and the road profile $\boldsymbol{r}(t)$, $\dot{\boldsymbol{r}}(t)$. Because the influence of the damage on the bridge vibrations is a kind of pulse, the impact of the damage on the bridge vibration is not transmitted strongly to the vehicle. The error term may affect the result, but the effect is constant and can be ignored. It is noted that the property, which affects SSMA, is the running speed of the vehicle, because the conversion process in Eqs. (4) depends on time space. From the above consideration, although **U**, the estimated bridge mode shape in Eqs. (16), is different from the actual value **A**, it can be used as an evaluation index for the bridge health. It also suggests that SSMA is a possible indicator for bridge screening, because it is more sensitive than the actual mode shape.

3 Methodology of Experiment

3.1 Experiment Details

The experiment time is 8:00 AM to 5:30 PM on May, 2022 except with Sunday and total took 3 weeks. The traffic is not regulated thus the data can include the other vehicle vibration. The weather contains rain and thunder. Temperature range is 8.0 to 27.4 degree Celsius based on the data of Japan Meteorological Agency.

The experiment vehicle parameter and details are shown Table 1 and Fig. 3. Vehicle weight is 13.8t including 6.8t addition weight by steel plate. The edge of crane is directed to back of vehicle. Wheelbase is 4850[mm] and the velocity range is assumed as 20-60[km/h]. Notice the experiment bridge includes shorter than wheelbase (Table 2) 4 point coordinates which is entrance or exit of bridge based on GIS. Notice this 4 points coordinates has error to real position or GPS. GPS device uses mosaic-HAT CLAS and set above the front wheel axle. 3axis accelerometer are set on unsprung front and rear wheel axle (total: 2 sensors). The ADC has 23bit/G resolution based on previous study

Table 1. Parameter of vehicle.

Name	Amount [Unit]
Vehicle Weight	13.8[t]
Wheelbase	4850[mm]
Velocity Range	20-60[km/h]
3axis Accelerometer (Unsprung)	F and R Total: 2 sensors.

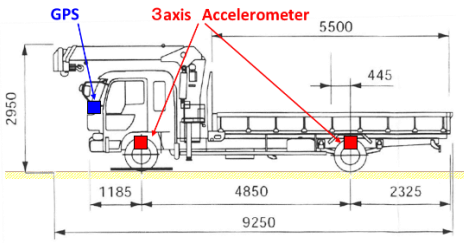

Fig. 3. The position of sensor on vehicle

Table 2. The experiment bridges.

No.	L	W	Span	Type	Year	No.	L	W	Span	Type	Year
1	30.7	20.2	2	PC	1984	55	35.1	11	1	PC	2005
2	5	34.8	1	Cal	1997	56	44	6.8	3	PC	1963
3	13.2	8.3	1	PC	1970	57	29.2	9.8	1	PC	1978
4	24.7	9.8	1	RCAr	1970	58	15.9	10.5	1	PC	1977
5	1.9	11.6	1	Cal	N/A	59	11.5	11	1	PC	1986
6	13.9	12.2	1	Cal	N/A	60	15.9	10.5	1	PC	1977
7	3.8	25.2	1	Cal	N/A	61	12.6	8.7	1	RC	1972
8	4.5	25	1	Cal	N/A	62	55	14.8	2	Steel	1970
9	2.1	25.2	1	Cal	N/A	63	24.8	10.3	1	Steel	1974
10	270	20.9	3	Steel	1996	64	9.4	7.5	1	PC	1972
11	34	11.5	1	PC	2012	65	24	7	2	RC	1965
12	105	18.8	7	PC	1970	66	10.1	7.5	1	PC	1966
13	10	7	1	PC	1957	67	22.7	7.3	1	Steel	1972
14	3.1	8.4	1	Cal	1972	68	276	8.7	3	PC	1974
15	3.6	8	1	RC	1972	69	5.8	15.1	1	Cal	1968
16	160	18.8	4	Steel	1969	70	17	8.4	2	PC	1963
17	18.2	10	1	Steel	1977	71	4.2	7.4	1	RC	1954
18	27	12.7	1	Steel	1974	72	4.8	11.3	1	RC	1981
19	10.1	13.6	1	RC	1934	73	33	16.8	1	Steel	1978
20	23	14	1	Steel	1971	74	7	20	1	Cal	1969
21	23	14	1	Steel	1971	75	9	27	1	Cal	1969
22	31	13.2	1	Steel	1972	76	4.8	13.4	1	Cal	N/A
23	31	13.2	1	Steel	1972	77	137	23.8	7	Hybrid	1989
24	29.1	10	2	PC	1989	78	8.8	10.8	1	PC	1987
25	16	8.2	1	PC	1980	79	6.9	9.8	1	RC	1929
26	330	11.9	8	Steel	1984	80	6	12.5	1	Cal	1983
27	330	11.9	8	Steel	1984	81	51.1	16	2	PC	1982
28	29.5	13.8	1	PC	1985	82	8.5	16.8	1	RC	1994
29	66.5	16.8	2	Steel	1985	83	62	12.7	2	RC	1989
30	8	13.4	1	RC	1982	84	21	12.5	1	PC	1994
31	5.4	6.8	1	RC	1960	85	37	16.7	2	PC	1966
32	10.6	9.1	1	RC	1952	86	20	25.8	1	PC	1983
33	7.3	12.5	1	Cal	1984	87	186.6	13.3	5	RC	1985
34	4.8	12.5	1	Cal	1978	88	66.6	13.8	4	PC	1986
35	44.3	8.7	2	PC	2009	89	24.1	9.8	2	PC	1978
36	174	12.8	7	PC	1997	90	18	12.7	1	PC	1997
37	4.5	12.1	1	RCRa	1992	91	29.3	12.8	1	RC	1987
38	36	11	2	PC	1983	92	16	8.2	1	PC	1980
39	2.9	12	1	RCRa	1991	93	7.9	8	1	PC	1966
40	22.5	18.8	1	PC	2006	94	13.6	7.5	1	PC	1967
41	89	15	3	PC	2013	95	5.6	11.8	1	RCRa	1992
42	3.5	12	1	RCRa	1991	96	45.1	11.4	2	Steel	1967
43	16	16.8	1	PC	1994	97	195	10.8	5	Steel	1989
44	30.88	9.02	1	PC	1973	98	3.7	11.5	1	RC	1962
45	11.5	11	1	PC	1986	99	72	12.8	2	Steel	1992
46	14	10.2	1	PC	1958	100	38	11.2	1	PC	1989
47	27.4	6.7	1	Steel	1967	101	29.2	32.8	1	Steel	1978
48	15	11.7	1	PC	1973	102	4.2	11.5	1	Cal	1977
49	9.2	8.8	1	RC	1977	103	180	8.5	5	Steel	2008
50	11	9.3	1	RC	1977	104	60.1	16.8	2	Steel	1986
51	264	10.8	9	PC	1989	105	6.5	12.6	1	Cal	1984
52	40	25.8	3	PC	1981	106	30.3	15	1	Steel	1976
53	39	25.8	1	PC	1981	107	16	8	1	PC	1980
54	2.5	12.5	1	RC	1983	108	10.7	7.5	1	Steel	1971

*RCAr: RC Arch, RCRa: RC Ramen, Cal: Calvert.

[6-8]. Sampling rate is 300[Hz].

The experiment is carried out on 108 bridges (Table 2). L is bridge length. The length range are 1.9-330[m]. W is bridge width and Span is the number of span. Type is bridge type of the structure and material. Especially, RCAr: RC Arch, RCRa: RC Ramen, Cal: Calvert. RC bridge is 23 contains 1 arch and 4 ramen, PC bridge is 44, Steel bridge is 24, and Calvert is 16. Notice this categories is not strict. All bridges doesn't have a fatal damage in regular inspection just before, and this study defined as almost healthy. No.45 is measured in previous experiments with different GPS accuracy [6-8]. In this experiment, No.45 are measured over 100 times. No.28, 33, 57, 74, 82, 89, 96 has only 1 data because of going through only or measurement failure. The others has 2 or more data. Multi-span bridges has 32. Although the original SSMA assumes to be applied to single span bridge data, this study verifies the data-driven method which calculate their SSMA as single span.

3.2 Data Verification

The acceleration data and the FFT result on No.45 is shown Fig. 4. In Fig. 4a, blue line is front, orange is rear. X axis is time[s], Y axis is acceleration[g]. No.45 has a step by joint at entrance and exit, and the impact peaks appear. The peaks of rear (orange) delay from front. The amplitude of rear around the middle of bridge is larger than front ones. This is assumed to be occurred by front is near center of gravity. In Fig. 4b, also blue line is front, orange is rear. X axis is frequency[Hz], Y axis is power spectrum density[$\mathrm{m}^2/\mathrm{s}^3$]. Y axis neglects under 5Hz because the effect of electrical trend is considered. The front has peaks around 13 and 25Hz, and the rear has peaks 8 and 30Hz. Considering the amplitude of rear over around the middle of bridge is larger, it is expected that rear is affected by bridge vibration, and front is by engine vibration.

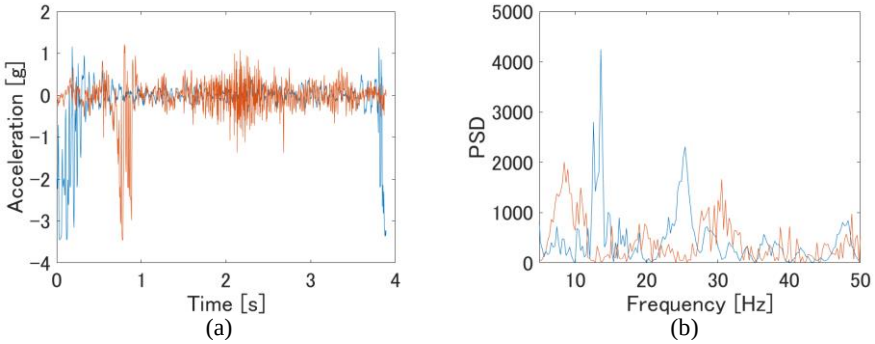

(a) (b)

Fig. 4. The acceleration of vehicle (a) and the FFT result (b).

4 Analysis and Discussion

Previous study suggested the relation of SSMA and bridge length [7]. The length - SSMA for all experiment bridges is shown Fig. 5 and 6. X axis is bridge length[m]. Y

axis is SSMA[deg.]. In Fig. 5, the trend between length – SSMA are suggested, especially, under 40m. Fig. 6 shows length – SSMA under 40m (92 bridges). The bridges under 40m are almost a single span. Some bridge has a large variance. This reason is suggested that they are affected by the environment of location (near the intersection

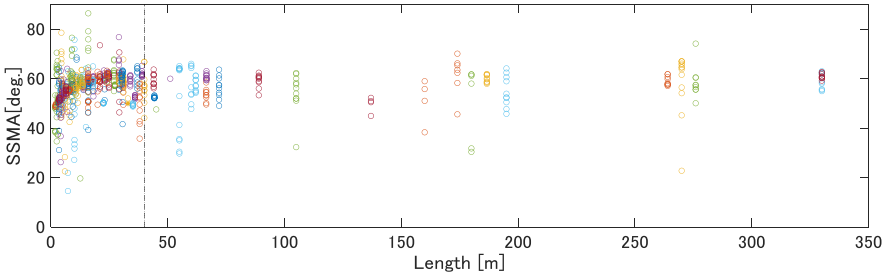

Fig. 5. The length – SSMA with all length range.

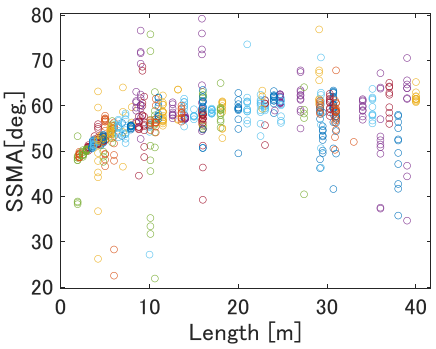

Fig. 6. The length – SSMA under 40m of bridge length.

etc…) in previous study [7-8]. Additionally, this study uses 4 point coordinates defined from GIS only which can be wrong, and the effect of error may increase in case of short span bridges. As the other reason, the bridge type is considered. For example, calvert bridges can be considered that calvert bridges may be interacted with the ground around bridge base and their behavior of vibration are different with others.

The trend curve is appeared to be bi-linear. The area in 0 to around 10m increase and over 10m is flat. This result may occurred by the relation of wheelbase and bridge length or calculation length. Because the calculation length is related to bridge length under the sample rate fixed, and the velocity has often a distribution curve such as a normal distribution, SSMA may have a trend corresponded to these conditions. On the other hands, this trend suggests that the screening method by SSMA can detect a damaged bridge without past data. The damage detection method in previous study using natural frequency or mode shape [1-4] ordinary need to compare the status of past data on health to latest. This proposal method may detect damage by using the distance between SSMA gained on unknown bridge and the trend curve. However, it should be considered that the trend curve can depend on the vehicle parameter, for example, weight.

5 Conclusion and Future Works

This study carried out the experiment to 108 bridges, and their SSMA trend is verified. The findings is as flow:

1. The SSMA shows that the length – SSMA has a trend appeared in previous study.
2. Some large variance of SSMA may be occurred with the location, position error or bridge type.
3. This trend suggests that the screening method by SSMA can detect a damaged bridge without past data because this method can use the distance between SSMA gained on unknown bridge and the trend curve instead of past data.

In future works, the analysis for bridge respectively is verified and it reveals the exclusion criteria such as the location near intersection, position error correction by GPS measurement on actual 4 point coordinates, and the effect from bridge types or vehicle weight. Additionally, this method can use DNN or RNN for improvement of detection accuracy or position error, and it validates how these method can apply.

References

1. Yang, Y.-B., Lin, C.W., Yau, J.D.: Extracting bridge frequencies from the dynamic response of a passing vehicle, Journal of Sound and Vibration, 272, 471-493 (2004).
2. Nagayama, T., Reksowardojo, A.P., Su, D., Mizutani. T.: Bridge natural frequency estimation by extracting the common vibration component from the responses of two vehicles, Engineering Structures, 150, 821-829 (2017).
3. Yang, Y.B., and Chang, K.C.: Extraction of bridge frequencies from the dynamic response of a passing vehicle enhanced by the EMD technique, Journal of Sound and Vibration, 322, 718-739 (2009).
4. Obrien, E. J., Malekjafarian, A.: A mode shape-based damage detection approach using laser measurement from a vehicle crossing a simply supported bridge, Structural Control Health Monitoring, 23(10), 1273-1286 (2016).
5. Yamamoto, K., and Ishikawa, M.: Numerical Verification of Bridge Screening Technology based on Vehicle Vibration, Lecture Notes in Engineering and Computer Science: Proceedings of The World Congress on Engineering 2016, 933-938, London, U.K (2016).
6. Takahashi, Y., Yamamoto, K.: The application of drive-by bridge damage detection based on continuous SSMA to the field experimental data, International Journal of Lifecycle Performance Engineering, 3(3-4), 310-330 (2019).
7. Takahashi, Y., Kaneko, N., Shin, R., Yamamoto, K.: The Validation of Sensor On-Vehicle for Evaluation of Actual Bridges with Signal Processing, Experimental Vibration Analysis for Civil Engineering Structures, Lecture Notes in Civil Engineering, 224, 631-642, Springer, Cham (2023).
8. Takahashi, Y., Kaneko, N., Shin, R., Yamamoto, K.: The Behavior Analysis of Spatial Singular Mode Angle Due to Addition of Noise to the Data in an Actual Bridge Experiment, European Workshop on Structural Health Monitoring, EWSHM 2022. Lecture Notes in Civil Engineering, 253, 690-699, Springer, Cham (2023).